LUDWIG-MAXIMILIANS-UNIVERSITÄT MÜNCHEN

Quantum Vacuum Simulation Program

A Numerical Scheme to Solve the Heisenberg-Euler Equations in 3+1 Dimensions

Baris Ölmez, Andreas Lindner, Hartmut Ruhl

FOR 2783, Yearly Retreat

LMU Munich, April 27, 2021

Bundesministerium
für Bildung
und Forschung

Abstract

A numerical scheme for solving the nonlinear Heisenberg-Euler equation in up to 3 spatial dimensions plus time is derived and its properties are discussed. This "quantum vacuum simulation algorithm" is tested against a set of already known analytical results and its power to go beyond analytically solvable scenarios is shown.

Based on

Pons Domenech, Arnau (2018): Simulation of quantum vacuum in higher dimensions. Dissertation, LMU München: Faculty of Physics

and

An implicit ODE-based numerical solver for the simulation of the Heisenberg-Euler equations in 3+1 dimensions

Overview

- Nonlinear Maxwell equations are stated
- Weak field expansion of the interaction Lagrangian is derived
- Matrix representation of Nonlinear Maxwell equations is presented
- Finite Difference method is presented and applied
- Dispersion relation is taken into account both analytically and numerically
- Simulation results in 1D and 2D are discussed

Theoretical Background

Nonlinear Maxwell Equations

Beforehand, the following electromagnetic and secular invariants

$$\mathcal{F} = -\frac{1}{4} F^{\mu\nu} F_{\mu\nu} = \frac{1}{2} \left(\frac{\vec{E}^2}{c^2} - \vec{B}^2 \right) , \qquad \mathcal{G} = -\frac{1}{4} F^{\mu\nu} \tilde{F}_{\mu\nu} = \frac{1}{c} \vec{E} \cdot \vec{B} \tag{1}$$

$$a = \sqrt{\sqrt{\mathcal{F}^2 + \mathcal{G}^2} + \mathcal{F}} , \qquad b = \sqrt{\sqrt{\mathcal{F}^2 + \mathcal{G}^2} - \mathcal{F}} \tag{2}$$

are used.
The Lagrangian for the quantum vacuum is the sum of the Maxwell and the Heisenberg-Euler Lagrangian

$$\mathcal{L} = \mathcal{L}_{\text{MW}} + \mathcal{L}_{\text{HE}} = \mathcal{F} + \mathcal{L}_{\text{HE}} . \tag{3}$$

Theoretical Background

From the Euler-Lagrange equations a system of four independent PDEs can be obtained

$$-\frac{1}{c}\partial_t\left(\vec{E}+c^2\partial_{\vec{E}}\mathcal{L}_{\text{HE}}\right)=\nabla\times\left(\vec{B}-\partial_{\vec{B}}\mathcal{L}_{\text{HE}}\right)\,, \tag{4}$$

where only the spatial components of the free index are taken into account. Comparing (4) with the macroscopic formulation of the Ampére law in Maxwells formulation leads to

$$\vec{P}=c^2\frac{\partial\mathcal{L}_{\text{HE}}}{\partial\vec{E}}\,,\quad \vec{M}=\frac{\partial\mathcal{L}_{\text{HE}}}{\partial\vec{B}}\,. \tag{5}$$

Theroretical Background

Weak-Field Expansion

Normalizing the electromagnetic invariants to the critical field strength yields

$$\mathcal{F} = -\frac{1}{4E_{\mathrm{cr}}^2} F^{\mu\nu} F_{\mu\nu} \,, \quad \mathcal{G} = -\frac{1}{4E_{\mathrm{cr}}^2} F^{\mu\nu} \tilde{F}_{\mu\nu} \,. \tag{6}$$

Using these definition the effective Lagrangian takes the form

$$\mathcal{L}_{\mathrm{HE}} = -\frac{m^4}{8\pi^2} \int_0^\infty ds \frac{e^{-s}}{s^3} \left(\frac{s^2}{3} \left(a^2 - b^2 \right) - 1 + abs^2 \cot(as) \coth(bs) \right) \,. \tag{7}$$

The cot and coth functions in (7) can be Taylor expanded around $as = bs = 0$.

Theoretical Background

Thus, inserting the Taylor expansions for $as\cot(as)$ and $bs\coth(bs)$ into (7) and performing the integral results in

$$\begin{aligned}\mathcal{L}_{\text{HE}} \approx \frac{m^4}{360\pi^2}\left(4\mathcal{F}^2 + 7\mathcal{G}^2\right) \\ + \frac{m^4}{630\pi^2}\left(8\mathcal{F}^3 + 13\mathcal{F}\mathcal{G}^2\right) \\ + \frac{m^4}{945\pi^2}\left(48\mathcal{F}^4 + 88\mathcal{F}^2\mathcal{G}^2 + 19\mathcal{G}^4\right) \\ + \frac{4m^4}{1485\pi^2}\left(160\mathcal{F}^5 + 332\mathcal{F}^3\mathcal{G}^2 + 127\mathcal{F}\mathcal{G}^4\right) .\end{aligned} \tag{8}$$

Theoretical Background

The first three terms in (8) are represented diagrammatically in the picture below.

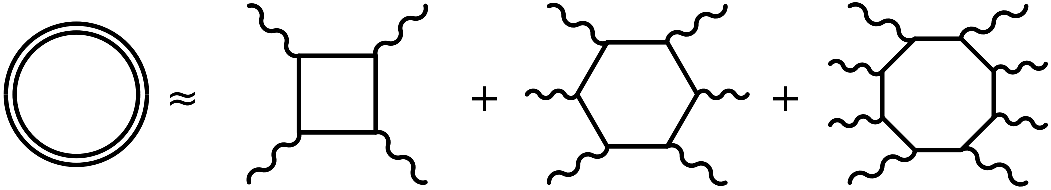

The simulation takes into account up to 6-photon processes in the weak field expansion

QVSP - Numerical Scheme

Reformulation of the Maxwell equations

For the rest of part one we set $\hbar = c = 1$.
Recalling the two modified Maxwell equations

$$\partial_t \vec{B} = -\nabla \times \vec{E}\,, \tag{9}$$

$$\partial_t \left(\vec{E} + \vec{P}\right) = \nabla \times \left(\vec{B} - \vec{M}\right)\,, \tag{10}$$

the first goal is to merge these equation and formulate a single PDE that describes the whole dynamics of the system.
The rotation of $\vec{M}$ can be rewritten as

$$\nabla \times \vec{M} = \begin{pmatrix} 0 & 0 & 0 \\ 0 & 0 & -1 \\ 0 & 1 & 0 \end{pmatrix} \partial_x \vec{M} + \begin{pmatrix} 0 & 0 & 1 \\ 0 & 0 & 0 \\ -1 & 0 & 0 \end{pmatrix} \partial_y \vec{M} + \begin{pmatrix} 0 & -1 & 0 \\ 1 & 0 & 0 \\ 0 & 0 & 0 \end{pmatrix} \partial_z \vec{M} \tag{11}$$

$$= \sum_{j \in \{x,y,z\}} \mathbf{Q}_j \partial_j \vec{M}\,. \tag{12}$$

QVSP - Numerical Scheme

Making use of the chain rule, the derivatives are given by

$$\partial_t \vec{P} = \mathbf{J}_{\vec{P}} \left(\vec{E} \right) \partial_t \vec{E} + \mathbf{J}_{\vec{P}} \left(\vec{B} \right) \partial_t \vec{B} \,, \tag{13}$$

where $\mathbf{J}$ is the Jacobi matrix. Therefore, the resulting PDE reads

$$\partial_t \vec{E} + \mathbf{J}_{\vec{P}} \left(\vec{E} \right) \partial_t \vec{E} + \mathbf{J}_{\vec{P}} \left(\vec{B} \right) \partial_t \vec{B} = \sum_{j \in \{x,y,z\}} \mathbf{Q}_j \left[-\mathbf{J}_{\vec{M}} \left(\vec{E} \right) \partial_j \vec{E} + \left(\mathbf{1}_3 - \mathbf{J}_{\vec{M}} \left(\vec{B} \right) \right) \partial_j \vec{B} \right] \,. \tag{14}$$

QVSP - Numerical Scheme

We introduce the electromagnetic vector $\vec{u}$ as

$$\vec{u} = \begin{pmatrix} \vec{E} \\ \vec{B} \end{pmatrix} \tag{15}$$

to rewrite the equation (14) as

$$\left(\left(\mathbf{1_3} + \mathbf{J}_{\vec{P}} \left(\vec{E} \right) \right) \quad \mathbf{J}_{\vec{P}} \left(\vec{B} \right) \right) \partial_t \vec{u} = \sum_{j \in \{x,y,z\}} \mathbf{Q}_j \left(\mathbf{J}_{\vec{M}} \left(\vec{E} \right) \quad \left(\mathbf{1_3} - \mathbf{J}_{\vec{M}} \left(\vec{B} \right) \right) \right) \partial_j \vec{u} \, . \tag{16}$$

Accordingly, equation (9) is given by

$$\left(\mathbf{0}_3 \quad \mathbf{1}_3 \right) \partial_t \vec{u} = - \sum_{j \in \{x,y,z\}} \mathbf{Q}_j \left(\mathbf{1}_3 \quad \mathbf{0}_3 \right) \partial_j \vec{u} \, . \tag{17}$$

QVSP - Numerical Scheme

Combining the equations (16) and (17) we arrive at

$$\left[\mathbf{1}_6 + \underbrace{\begin{pmatrix} \mathbf{J}_{\vec{P}}\left(\vec{E}\right) & \mathbf{J}_{\vec{P}}\left(\vec{B}\right) \\ \mathbf{0}_3 & \mathbf{0}_3 \end{pmatrix}}_{\mathbf{A}}\right] \partial_t \vec{u} = \sum_{j\in\{x,y,z\}} \underbrace{\begin{pmatrix} -\mathbf{Q}_j \mathbf{J}_{\vec{M}}\left(\vec{E}\right) & \mathbf{Q}_j - \mathbf{Q}_j \mathbf{J}_{\vec{M}}\left(\vec{B}\right) \\ -\mathbf{Q}_j & \mathbf{0}_3 \end{pmatrix}}_{\mathbf{B}_j} \partial_j \vec{u} \tag{18}$$

$$\left(\mathbf{1}_6 + \mathbf{A}\right) \partial_t \vec{u} = \sum_j \mathbf{B}_j \partial_j \vec{u}\,. \tag{19}$$

Note, that (19) contains the full dynamics of the electromagnetic fields.

Finite Differences

The Taylor series of a function $f(x + k\Delta x)$ is

$$f(x + k\Delta x) = f(x) + \Delta x k f'(x) + \frac{1}{2}(\Delta x k)^2 f''(x) + \frac{1}{6}(\Delta x k)^3 f'''(x) + \dots . \qquad (20)$$

In matrix notation for $k \in \{-4, -3, ..., 3, 4\}$ (20) becomes

$$\begin{pmatrix} f(x-4\Delta x) \\ f(x-3\Delta x) \\ f(x-2\Delta x) \\ f(x-\Delta x) \\ f(x) \\ f(x+\Delta x) \\ f(x+2\Delta x) \\ f(x+3\Delta x) \\ f(x+4\Delta x) \end{pmatrix} \approx \frac{1}{120} \begin{pmatrix} 120 & -480 & 960 & -1280 & 1280 & -1024 \\ 120 & -360 & 540 & -540 & 405 & -243 \\ 120 & -240 & 240 & -160 & 80 & -32 \\ 120 & -120 & 60 & -20 & 5 & -1 \\ 120 & 0 & 0 & 0 & 0 & 0 \\ 120 & 120 & 60 & 20 & 5 & 1 \\ 120 & 240 & 240 & 160 & 80 & 32 \\ 120 & 360 & 540 & 540 & 405 & 243 \\ 120 & 480 & 960 & 1280 & 1280 & 1024 \end{pmatrix} \begin{pmatrix} f(x) \\ \Delta x f'(x) \\ (\Delta x)^2 f''(x) \\ (\Delta x)^3 f'''(x) \\ (\Delta x)^4 f''''(x) \\ (\Delta x)^5 f'''''(x) \end{pmatrix} . \qquad (21)$$

Numerical Mathematics

From (21) the upwind biased finite difference approximation for the first derivative can be derived. We obtain

$$f'_{(1,0)}(x) = \frac{f(x + \Delta x) - f(x)}{\Delta x}\,, \tag{22}$$

where the corresponding coefficients are 1 for $k = 1$ and -1 for $k = 0$. The indices m and n denote the lowest and highest considered values of k. More generally, the first derivate of f yields

$$\mathcal{D}f = f'_{(n,m)}(x) = \frac{1}{\Delta x} \sum_{k=n}^{m} \mathcal{S}_k f(x + k\Delta x)\,. \tag{23}$$

The indices m and n denote the lowest and highest considered values of k. $\mathcal{S}$ is the derivative stencil. First order derivative stencil for finite differences is depicted below.

Numerical Mathematics

First order derivative stencil for finite differences is depicted below.

$\mathcal{O} = 1$	-1	0	1
	-1	1	
		-1	1

$\mathcal{O} = 2$	-2	-1	0	1	2
	0.5	-2	1.5		
		-0.5	0	0.5	
			-1.5	-2	-0.5

Here, forward and backward differences are taken into account.

From PDE to ODE

Recalling (19) and multiplying both sides by $(\mathbf{1}_6 + \mathbf{A})^{-1}$ yields

$$\partial_t \vec{u} = (\mathbf{1}_6 + \mathbf{A})^{-1} \sum_j \mathbf{B}_j \partial_j \vec{u} \,. \tag{24}$$

Henceforth, for simplicity the linear case is discussed. Thus, the matrices in (18) become

$$\mathbf{A} = 0 \,, \quad \mathbf{B}_j = \begin{pmatrix} \mathbf{0}_3 & \mathbf{Q}_j \\ -\mathbf{Q}_j & \mathbf{0}_3 \end{pmatrix} \tag{25}$$

so that (24) can be reformulated as

$$\partial_t \vec{u} = \sum_j \begin{pmatrix} \mathbf{0}_3 & \mathbf{Q}_j \\ -\mathbf{Q}_j & \mathbf{0}_3 \end{pmatrix} \partial_j \vec{u} \,. \tag{26}$$

QVSP - Numerical Scheme

Furthermore, for the diagonalization of $\mathbf{B}_j$ we make use of the rotation matrices for each space direction

$$\mathbf{R}_x = \frac{1}{\sqrt{2}} \begin{pmatrix} 0 & 0 & 0 & 0 & 0 & 1 \\ -1 & 0 & 1 & 0 & 0 & 0 \\ 0 & 1 & 0 & -1 & 0 & 0 \\ 0 & 0 & 0 & 0 & 1 & 0 \\ 0 & 1 & 0 & 1 & 0 & 0 \\ 1 & 0 & 1 & 0 & 0 & 0 \end{pmatrix}, \quad \mathbf{R}_y = \frac{1}{\sqrt{2}} \begin{pmatrix} 1 & 0 & -1 & 0 & 0 & 0 \\ 0 & 0 & 0 & 0 & 0 & 1 \\ 0 & -1 & 0 & 1 & 0 & 0 \\ 0 & 1 & 0 & 1 & 0 & 0 \\ 0 & 0 & 0 & 0 & 1 & 0 \\ 1 & 0 & 1 & 0 & 0 & 0 \end{pmatrix},$$

QVSP - Numerical Scheme

$$\mathbf{R}_z = \frac{1}{\sqrt{2}} \begin{pmatrix} -1 & 0 & 1 & 0 & 0 & 0 \\ 0 & 1 & 0 & -1 & 0 & 0 \\ 0 & 0 & 0 & 0 & 0 & 1 \\ 0 & 1 & 0 & 1 & 0 & 0 \\ 1 & 0 & 1 & 0 & 0 & 0 \\ 0 & 0 & 0 & 0 & 1 & 0 \end{pmatrix}, \tag{27}$$

since they are defined as

$$\mathbf{B}_j = \mathbf{R}_j \mathrm{diag}(1, 1, -1, -1, 0, 0) \mathbf{R}_j^\mathsf{T} . \tag{28}$$

The derivation in space of $\vec{u}$ can be rewritten as

$$\partial_j \vec{u} = \mathbf{R}_j \partial_j \mathbf{R}_j^\mathsf{T} \vec{u} \tag{29}$$

or for the case of one space direction (e.g. x-direction)

$$\partial_x \vec{u} = \mathbf{R}_x \partial_x \mathbf{R}_x^\mathsf{T} \vec{u} . \tag{30}$$

QVSP - Numerical Scheme

As derived above the spatial derivative can be replaced by the finite sum which is weighted by the derivative stencil (23). Without loss of generality we obtain

$$\partial_x \vec{u}(x, y, z) \approx \mathbf{R}_x \mathcal{D}_x \mathbf{R}_x^\top \vec{u}(x, y, z) = \mathbf{R}_x \sum_\nu \frac{1}{\Delta_x} S_\nu \left(\mathbf{R}_x^\top \vec{u} \right) (x + \nu \Delta x, y, z) \,, \tag{31}$$

where the stencil matrices for the lowest order are given by

$$S_{-1} = \mathrm{diag}(-1, -1, 0, 0, -\frac{1}{2}, -\frac{1}{2}) \tag{32}$$

$$S_0 = \mathrm{diag}(1, 1, -1, -1, 0, 0) \tag{33}$$

$$S_1 = \mathrm{diag}(0, 0, 1, 1, \frac{1}{2}, \frac{1}{2}) \,. \tag{34}$$

QVSP - Numerical Scheme

Considering all three directions the resulting ODE reads

$$\partial_t \vec{u} = (\mathbf{1}_6 + \mathbf{A})^{-1} \sum_{j \in \{x,y,z\}} \mathbf{B}_j \mathbf{R}_j \sum_{\nu} \frac{1}{\Delta_j} S_\nu \mathbf{R}_j^\mathsf{T} \vec{u}_{j+\nu} \,. \tag{35}$$

The equation (35) is solved with the help of the CVODE library which is a part of the Sundials distribution.

QVSP - Numerical Scheme

Dispersion Relation

For simplicity we are neglecting nonlinearities for the further investigation of the dispersion relation. The analytical properties of the numerical scheme can be analyzed by picking a plane wave ansatz

$$\vec{E}(\vec{x}, t) = \vec{E}_0 e^{-i\left(\omega t - \vec{k}\cdot\vec{r}\right)}, \tag{36}$$

where $\vec{E}_0$ is the amplitude and polarization vector. To do so, the plane wave ansatz can be inserted into (35) so that we arrive at

$$0 = \det\left(i\omega \mathbf{1}_6 + \sum_{j\in\{x,y,z\}} \mathrm{adiag}(\mathbf{Q}_j, -\mathbf{Q}_j)\mathbf{R}_j^T \sum_{\nu} S_\nu^j e^{-i\nu k_j \Delta_j} \mathbf{R}_j \right). \tag{37}$$

where S^j are identical in all spatial dimensions.

Analytical Dispersion Relation

- For small $k \cdot \Delta$ everything is fine.
- Superluminar phase velocity at $k \cdot \Delta \simeq \pi/2$
- For $k \cdot \Delta \gtrsim \pi/2$ the imaginary part of ω causes a damping
- *Nyquist frequency* at $k = \pi$

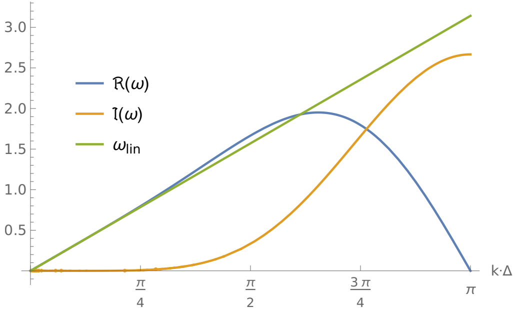

A. Domenech and H. Ruhl, arXiv:1607.00253, 2017

Numerical Check of the Dispersion Relation

- Plane wave propagating through the vacuum
- Grid Resolution: 2D lattice with length 80 µm divided into 1024×1024 points $\Rightarrow \Delta^{-1} = 128 \times 10^5\,\mathrm{m}^{-1}$
- For $f \leq 1 \times 10^6\,\mathrm{m}^{-1}$ (rightmost value in top figure, plot in bottom figure) everything is fine at this resolution.

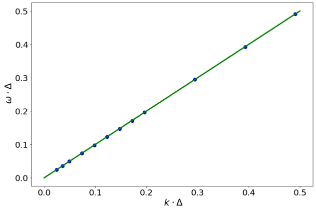

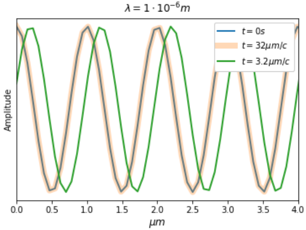

QVSP Dispersion Relation

Numerical Check of the Dispersion Relation Nyquist Frequency

- We observe the damping and superluminous effect at half the Nyquist frequency after a relevant amount of time
- Quick annihilation at the Nyquist frequency, $f_{\mathrm{Ny}} = \Delta^{-1}/2 = 6.4 \times 10^{6}\ \mathrm{m}^{-1}$
- Beyond f_{Ny} waves cannot be modeled adequately anymore
- Of course, there is always the possibility to increase the grid (and time) resolution if the computer allows it

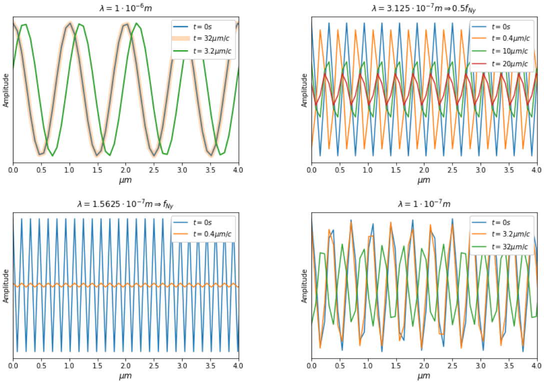

QVSP Computational Complexity

Scaling of the Computational Complexity

- Calculation of derivatives for each point and every dimension

$$\mathcal{C} \sim N_x \cdot N_y \cdot N_z \cdot D$$

- Evaluation of (24) for each lattice point

$$\mathcal{C} \sim N_x \cdot N_y \cdot N_z \cdot (D + 1)$$

- CVODE solver dependence on precision

$$\mathcal{C} \sim N_x \cdot N_y \cdot N_z \cdot \Delta^{-1}$$

- Total scaling

$$\mathcal{C} \sim N_x \cdot N_y \cdot N_z \cdot \Delta^{-1} \cdot (D + 1)$$

Simulation Results in 1D

- Phase Velocity in a Strong Background
- Polarization Flipping
- High Harmonic Generation

Phase Velocity Variation in a Strong Electromagnetic Background

Propagate a plane wave through a linearly polarized electromagnetic background of different field strengths

- Background field strengths are varied as well as the relative orthogonal polarization from parallel to orthogonal
- Wavevector from here on normalized to $|\vec{k}| = 1/\lambda$

Grid	Length	100 μm
	Lattice Points	1000
Background	Amplitude Vector	(0,60,0) μE_{cr} to (0,1.5,0)E_{cr}
	Wavevector	(-1,0,0)Pm^{-1}
Probe	Amplitude Vector	(0,1,0) and (0,0,1) μE_{cr}
	Wavevector	(0.5,0,0) $\mu\mathrm{m}^{-1}$

Change of refractive index by vacuum birefringence ⇒

Phase Velocity Variation in a Strong Electromagnetic Background

- Refractive index for orthogonal (+) and parallel (-) relative polarization

$$n_{\pm} = 1 + \frac{\alpha}{45\pi}(11 \pm 3)\frac{E^2}{E_{cr}^2} = 1 + \delta n_{\pm}$$

- Theoretical:

$$v \rightarrow \frac{1}{1+\delta n_{\pm}} \Rightarrow v_{nli} = -\frac{\delta n_{\pm}}{1+\delta n_{\pm}}$$

- Numerical:

$$v_{nli} = -\frac{1}{2\pi m}\arg\left(\mathrm{FT}[E_z(x,t_m)](\lambda^{-1})\right) \;,\; t_m = m\lambda$$

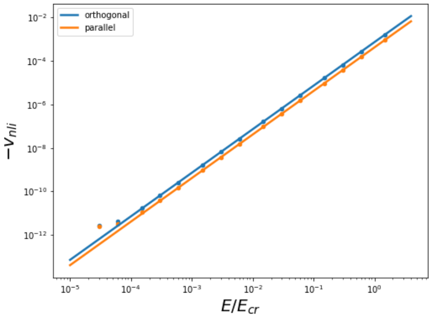

$\Rightarrow$Numerical errors for $E < E_{cr} 1 \times 10^{-4}$

V. Dinu, T. Heinzl, A. Ilderton, M.Marklund, G. Torgrimsson, Physical Review D, 2014
A. Domenech, LMU, 2018

Polarization Flipping – Vacuum Birefringence

- Different refractive indices for polarizations $\vec{\varepsilon}_{\parallel}$ and $\vec{\varepsilon}_{\perp}$ (don't confuse with $\mp$ from previous slide)
- Different speeds of parallel and perpendicular components
- **Bi**refringence

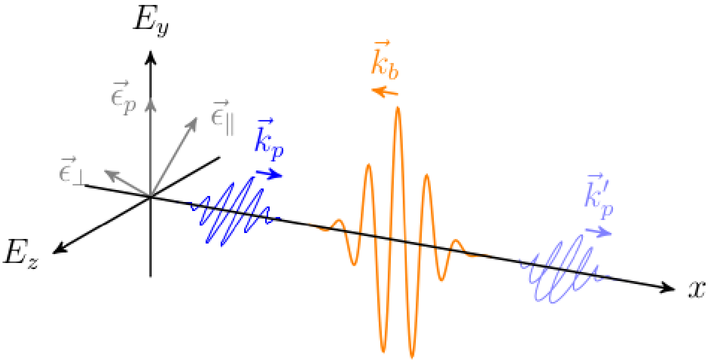

Polarization Flipping – Vacuum Birefringence

- 1D Gaussian pulses with $\vec{E} = \vec{A}\, e^{-(\vec{x}-\vec{x}_0)^2/\tau^2} \cos(2\pi \vec{k} \cdot \vec{x})$
- Parallel is $\vec{\varepsilon}_{\parallel} = 1/\sqrt{2}\,(0, 1, 1)$
- Perpendicular is $\vec{\varepsilon}_{\perp} = 1/\sqrt{2}\,(0, -1, 1)$
- The probe wavevectors used in the simulations need be much smaller - we have to extrapolate

Grid	Length	80 μm
	Lattice Points	$\simeq 1 \times 10^7$
Pump	Amplitude Vector	(0,0,0.34) mE_{cr}
	Wavevector	(-1.25,0,0) μm^{-1}
	Center	58 μm
	Width	30 fs
Probe	Amplitude Vector	(0,50,50) μE_{cr}
	Wavevector	(10.4,0,0) nm^{-1}
	Center	22 μm
	Width	30 fs

Benchmark: F. Karbstein, H. Gies, M. Reuter, and M. Zepf, Physical Review D, 2015

Polarization Flipping Vacuum Birefringence

Initial setting (sketch)

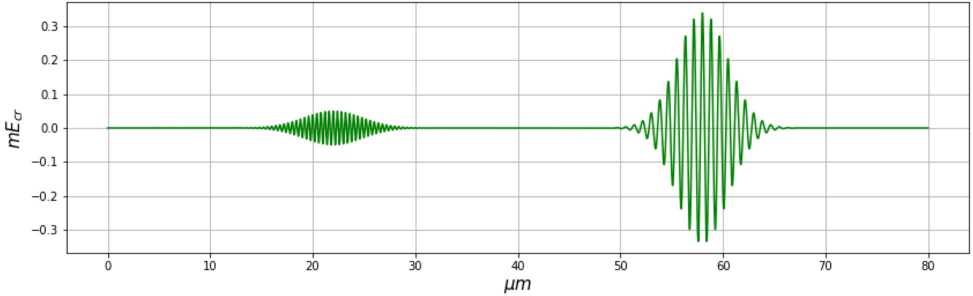

Analysis of Polarization Flips

Overall check of the flipping probability given in the low energy regime ($k_p k_b << m^2$) by

$$P_{\text{flip}} = \frac{\alpha^2}{255\lambda^2} \sin^2(2\sigma) \left(\int dx \frac{E_b(x)^2}{E_{cr}^2} \right)^2 \tag{38}$$

via the ratio of flipped quanta obtained through the field energies and strengths by

$$\frac{N_\perp}{N} = \frac{N_\perp \hbar\omega}{N\hbar\omega} = \frac{\mathcal{E}_\perp}{\mathcal{E}} \text{, with } \mathcal{E}_\perp = \sum_{x_i} \left(\vec{E}(x_i) \cdot \vec{\varepsilon}_\perp \right)^2$$

See also V. Dinu, T. Heinzl, A. Ilderton, M.Marklund, G. Torgrimsson, Physical Review D, 2014

QVSP 1D Simulations

Analysis of Polarization Flips

- Dependency on the pump field strength
- Dependency on the probe wavelength
- Extrapolation to small wavelengths due to heavy simulations

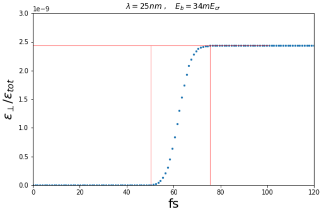

- Flipping process can be time-resolved by the simulation

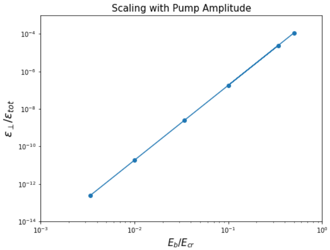

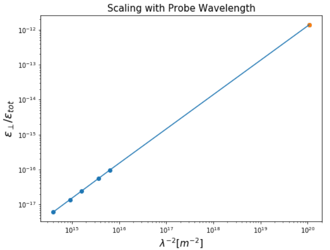

Analysis of Polarization Flips

- Need to refine the analysis

(Near-) Future work:

- Check of other dependencies in (38): dependency on polarization shift, independence of pulse shapes

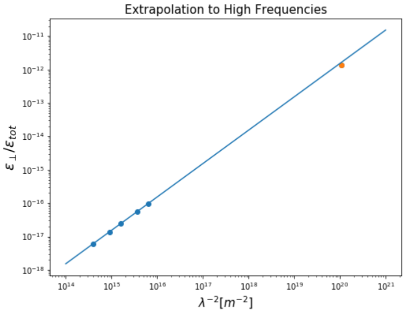

High Harmonic Generation

Effective higher order scattering of **p**robe and **b**ackground photons

- Energy conservation at the effective vertices can result in higher harmonics via photon merging
- In the following: $\omega_b = 0$ (zero-frequency background)
- On a later slide: Two non-zero frequency pulses and collision at an angle

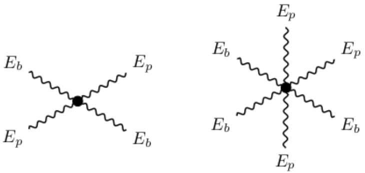

Effective vertices for 4- and 6-photon scattering

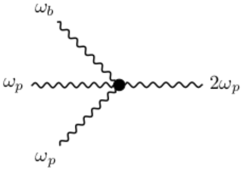

High harmonic generation

High Harmonic Generation Initial Settings

- Zero-frequency background

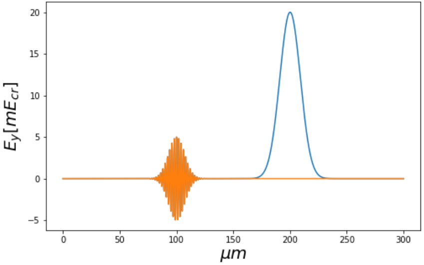

Grid	Length	300 µm
	Lattice Points	4000
Pump	Amplitude Vector	(0,20,0) mE_{cr}
	Wavevector	(-1,0,0) m^{-1}
	Center	200 µm
	Width	12.8 µm
Probe	Amplitude Vector	(0,5,0) mE_{cr}
	Wavevector	(0.5,0,0) μm^{-1}
	Center	100 µm
	Width	10 µm

B. King, P. Böhl, and H. Ruhl, Physical Review D, 2014
P. Böhl, LMU, 2016

High Harmonics Analysis

Logarithmic scale makes harmonics visible in frequency space

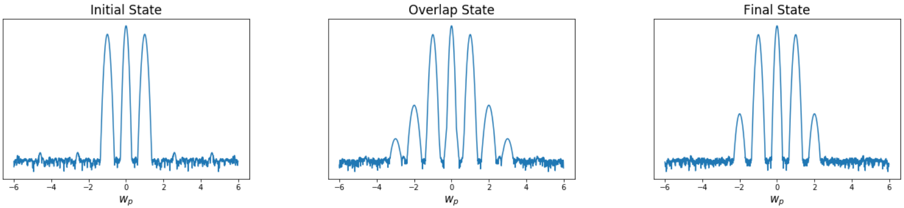

- Only 2nd harmonic is an asymptotic higher harmonic

QVSP 1D Simulations

(High) Harmonics Analysis

- Harmonics are analysed by subtracting classical linear vacuum propagation from nonlinear propagation
- Only signals generated by nonlinearities left
- Get rid of main signals for $\omega = 0$ and $\omega = \omega_p$ (dc component and fundamental harmonic)

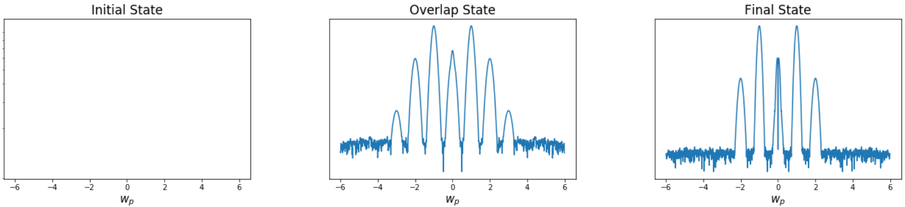

- Extraction of harmonic amplitudes: Filter desired frequency in Fourier space and transform back to position space.

(High) Harmonics Analysis

- Amplitude of the harmonics (linear vacuum subtracted) against time
- Small systematic error by back and forth Fourier transformations
- 0th and 3rd harmonic purely by 6-photon processes
- To do: Add analytical results

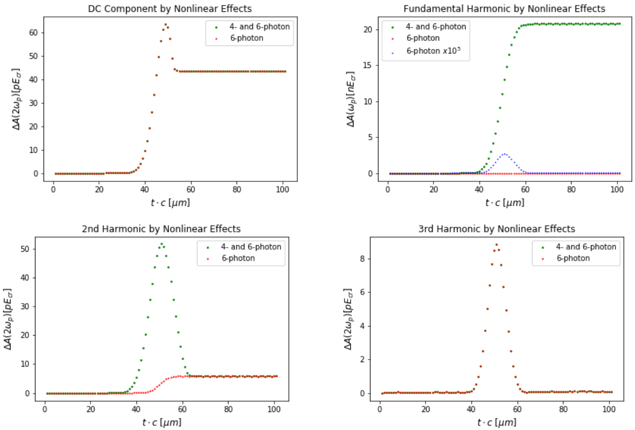

Simulation Results in 2D

- Quasi-1D: Coaxial Pulses
- Perpendicular Pulses and Odd Angles
- Orthogonally Polarized Pulses

Rough Settings

- Two equal 2D Gaussian Pulses in a square
- Degeneracy of harmonic signals only for $\vec{k}_p = \pm\vec{k}_b$
- Varying relative propagation direction to get rich diversity of signals
- Check of both parallel and orthogonal relative polarizations

Grid	Size	80 µm x 80 µm
	Lattice Points	1024 x 1024
Pulse 1	Amplitude Vector	(0,0,50) mE_{cr}
	Wavevector	(1,0,0) µm^{-1}
	...	
Pulse 2	Amplitude Vector	(0,0,50) mE_{cr}
	Wavevector	(-1,0,0) µm^{-1}
	...	

Coaxial Pulses

Position Space (top) and Frequency Space (bottom)

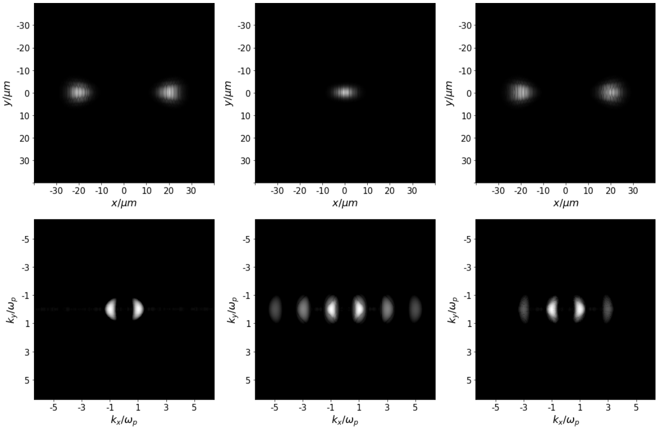

E_z-components

- $\vec{k}_p = -\vec{k}_b$
- 3ω and 5ω signals in the overlap field and a weak 3ω signal in the asymptotic field
- Asymptotic signals due to 6-photon scattering only

Coaxial Pulses Relation to 1D Case

Similar to 1D:

- asymptotic high harmonics due to 6-photon diagrams

But:

- Sharpening of the asymptotic pulse (hardly visible), according broadening of the ω signals
- Reason: Birefringence effects are stronger in the center of the pulse.
- Post-collision pulses are sharper in position space and broader in frequency domain.

Perpendicular Pulses

- Variety of mixing signals by repeal of degeneracy (mostly non-asymptotic 4-photon processes)
- 5-photon merging channels clearly visible
- Nearly all signals vanish in the far field again
- Asymptotic harmonics propagate along the axes only

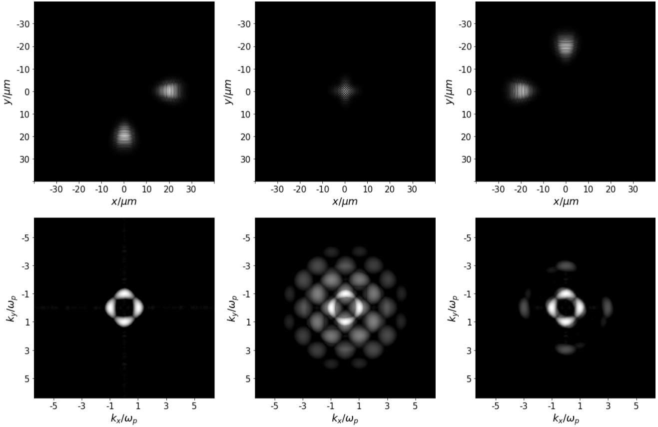

E_z-components

Perpendicular Pulses Relation to 1D Case

Similar to 1D:

- asymptotic high harmonics due to 6-photon diagrams

But:

- Symmetry axis is neither $k_x = 0$ nor $k_y = 0$ but $k_x + k_y = 0$ $\Rightarrow$initial symmetry of the system
- Birefringence effects (broadening) no longer symmetric in the far field $\Rightarrow$keep total momentum constant as well as invariance under boost trafos

Odd Angle

Pulses colliding at an angle of 135°

- Like a boost transformation of perpendicular case

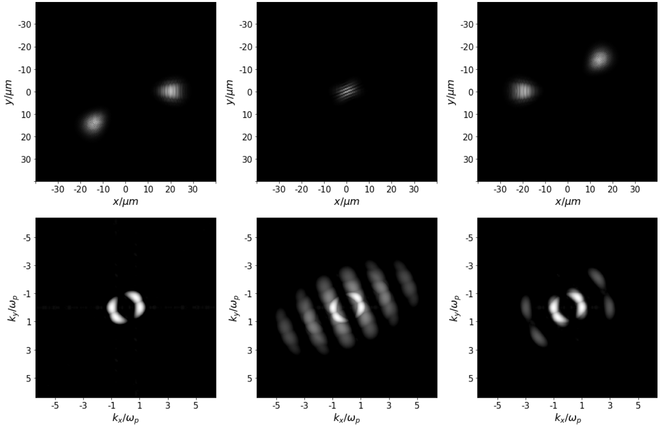

E_z-components

QVSP 2D Simulations

Orthogonal Polarization

k-space of pulses colliding at an angle of 90° and 135°

- Only one of the pulses is polarized along E_z, whose frequency space is shown here
- Momentum conservation: Signals have the polarisation of the pulse that contributes an odd amount of photons

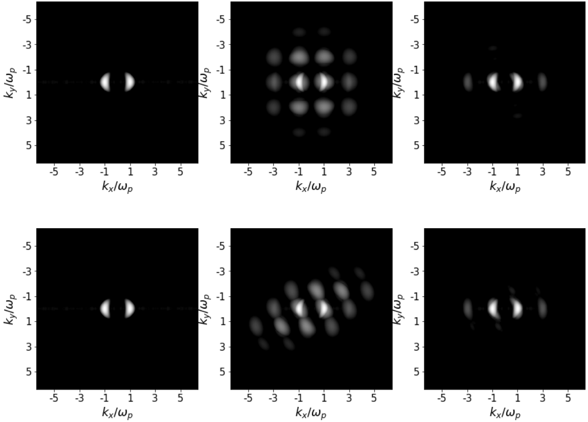

E_z-components (the one pulse)

Orthogonal Polarization

k-space of pulses colliding at an angle of 90° and 135°

- Here frequency space of B_z-components (from the pulse polarized along E_y)

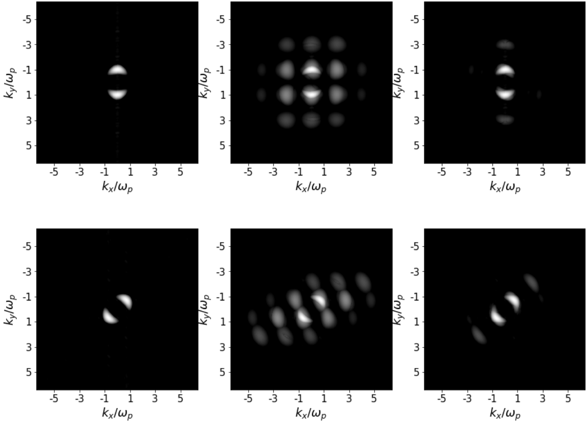

B_z-components (the other pulse)

QVSP Summary

- An ODE-based numerical solver for nonlinear wave equations in 3+1 dimensions is presented
- The solver is applied to the Heisenberg-Euler equations in weak field expansion but is not limited to them
- The dispersion relation annihilates unphysical modes
- The phase velocity varies correctly in a strong electromagnetic background
- A backtesting of polarization flipping and higher-harmonic generation phenomena in 1D is performed
- Simulations allow the interpretation of non-analytically solvable 2D scenarios containing these effects

QVSP Conclusions

Deficiencies Scale Restriction

- Field strengths are restricted to below critical values
- Fields ought to vary on much larger scale than Compton of electron
- Instead of probe *quanta*, can only simulate pulses
- Restriction to purely photonic processes no pair creation etc.

Caveats and Hurdles

- Attention to fine enough grid resolution and accompanying computational complexity
- Simulation output is field components of all pulses combined
  $\Rightarrow$potentially arduous post-processing to filter desired signals

QVSP Conclusions

Benefits (Almost) Complete Picture in a Simulation

- Numerical simulation can show all vacuum effects *simultaneously*
- Time-resolve all different processes
- Directly applicable to real world experimental settings with easily adaptable configurations
- **Heisenberg-Euler Solver!**

Outlook

- Publication of the results
- Adaptive grids
- Tomographic methods for strong pulse characterization
- Make code scalable for 3D simulations
- Support our colleagues with simulations

Thank you